J. Fluid Mech. (1997), *vol.* 350, *pp.* 351–374. Printed in the United Kingdom

Non-isotropic dissipation in non-homogeneous turbulence

By MARTIN OBERLACK

Institut für Technische Mechanik, RWTH Aachen, 52056 Aachen, Germany

(Received 20 July 1995 and in revised form 9 July 1997)

On the basis of the two-point velocity correlation equation a new tensor length-scale equation and in turn a dissipation rate tensor equation and the pressure–strain correlation are derived by means of asymptotic analysis and frame-invariance considerations. The new dissipation rate tensor equation can account for non-isotropy effects of the dissipation rate and streamline curvature. The entire analysis is valid for incompressible as well as for compressible turbulence in the limit of small Mach numbers. The pressure–strain correlation is expressed as a functional of the two-point correlation, leading to an extended compressible version of the linear formulation of the pressure–strain correlation. In this turbulence modelling approach the only terms which still need *ad hoc* closure assumptions are the triple correlation of the fluctuating velocities and a tensor relation between the length scale and the dissipation rate tensor. Hence, a consistent formulation of the return term in the pressure–strain correlation and the dissipation tensor equation is achieved. The model has been integrated numerically for several different homogeneous and inhomogeneous test cases and results are compared with DNS, LES and experimental data.

1. Introduction

Current second-moment closure models still suffer from three unresolved problems: the closure of the velocity–pressure-gradient correlation Ψ_{ij}, the triple correlation ${}^{\mathrm{t}}D_{ij}$ and the dissipation rate tensor ε_{ij}. The velocity–pressure-gradient correlation is split into the pressure–strain correlation Φ_{ij} and the pressure–diffusion ${}^{\mathrm{p}}D_{ij}$ which is modelled together with the triple correlation as a gradient-type diffusion term.

A significant amount of information that is needed for the closure of these terms is contained in the two-point correlation tensor R_{ij}. Given R_{ij}, one can express the Reynolds stress tensor, the dissipation rate tensor, and the rapid part of the pressure–strain tensor (without the wall term) as a functional of R_{ij}:

$$\overline{u_i u_j} = R_{ij}(\boldsymbol{x}, \boldsymbol{r} = 0),$$

$$\varepsilon_{ij} = \lim_{r \to 0} \nu \left[\frac{\partial^2 R_{ij}}{\partial x_k \partial r_k} - \frac{\partial^2 R_{ij}}{\partial r_k \partial r_k} \right],$$

$$\Phi_{ij}^{rapid} = \frac{1}{2\pi} \int_V \frac{\partial \bar{u}_k}{\partial x_l}(\boldsymbol{x} + \boldsymbol{r}) \left(\frac{\partial^2 R_{il}}{\partial x_j \partial r_k} - \frac{\partial^2 R_{il}}{\partial r_j \partial r_k} \right) \frac{\mathrm{d}^3 r}{|\boldsymbol{r}|} + (i \leftrightarrow j),$$

where $(i \leftrightarrow j)$ indicates the addition of the previous term with interchanged indices i and j. R_{ij} also provides turbulence length-scale information, including the integral length scale and the Taylor microscale.

For engineering applications it is impractical to solve the two-point correlation equations to get the required one-point information. The approach should be to extract information from the two-point correlation equations in order to improve one-point models.

A first step was made by von Kármán & Howarth (1938) who analysed the two-point correlation equation for isotropic turbulence, which gave early insight into the decay of isotropic turbulence and the evolution of turbulent length scales. The form of the isotropic two-point correlation tensor introduced by von Kármán & Howarth (1938) was used by Crow (1968) to derive a first approximation of the rapid pressure–strain correlation. A crucial further step was made by Naot, Shavit & Wolfshtein (1973), who extended the isotropic tensor form for R_{ij} to a quasi-isotropic model, which led to the linear rapid pressure–strain model utilized in the well-known Launder, Reece & Rodi (1975) second-moment closure model, referred to below as LRR model. Lin & Wolfshtein (1979) further extended this approach to a nonlinear model, but did not retain any nonlinear terms in the pressure–strain model.

Even though it is more solid to base the pressure–strain correlation on the two-point correlation function, nearly all of the most common models for the pressure–strain term are modelled as an algebraic function of local turbulence parameters, in particular the Reynolds stress anisotropy tensor b_{ij} and its invariants, the mean flow gradient and a scalar length scale (Launder *et al*. 1975; Lumley 1978; Rotta 1951*a*). Lumley & Newman (1977) suggested absorbing all non-isotropic effects of ε_{ij}, namely d_{ij}, into the pressure–strain correlation Φ_{ij}.

In addition to the turbulent diffusion and the pressure–strain correlation one-point turbulence models require some sort of length-scale information, which in the most common turbulence models is given by a scalar dissipation rate equation. Many common dissipation rate function models are based on scalar transport equations that are variations of the scalar dissipation rate equation first proposed by Hanjalić & Launder (1972). This approach can be traced back to Kolmogorov's inertial subrange theory (Kolmogorov 1941) in which the dissipation is proposed to be locally isotropic in the limit of large Reynolds numbers. Hence, the dissipation process is solely determined by the scalar dissipation ε and the tensorial character of the dissipation rate function is modelled as an isotropic tensor $\varepsilon_{ij} = (\delta_{ij}/3)\varepsilon$.

The deficiencies of the classical scalar dissipation rate models are largely related to the scalar ε-equation, the reasons being manifold. First, deriving a closed ε-equation from basic principles is difficult. It is mainly an empirical equation, since many complicated terms have to be modelled. Second, in its classical formulation the dissipation rate equation cannot account for strong streamline curvature or Coriolis effects. Third, data from direct numerical simulations have revealed the strong non-isotropic nature of the dissipation process (Bardina, Ferziger & Reynolds 1983; Kim, Moin & Moser 1987; Lee & Reynolds 1985). The experimental evidence for the local isotropy assumption has been debated. Recent flat-plate boundary layer experiments of Saddoughi & Veeravalli (1994) support Kolmogorov's hypothesis of isotropy. However, other experiments, e.g. Tavoularis & Corrsin (1984), clearly find anisotropic small scales. On the other hand, there is theoretical evidence based on the exact dissipation rate tensor equation that the dissipation process may not be locally isotropic for large mean rates of strain (Durbin & Speziale 1991). Local isotropy may not be valid even in the limit of large Reynolds numbers. A different investigation, but coming to the same conclusions, has been done by Brasseur & Yeung (1991) and Brasseur (1991). They analysed the Navier–Stokes equations in Fourier space and came to the following conclusion: in a turbulent flow the coupling between the large

and the small scales persists and is dynamically significant in the infinite-Reynolds-number limit. Hence, anisotropy of the small-scales can be induced by the anisotropy of the large scales. In fact, a finite level of small-scale anisotropy must always exist if the large scales are anisotropic.

There have been several attempts to model a dissipation rate tensor either as an algebraic function as suggested e.g. by Hallbäck, Groth & Johansson (1994) or as a dissipation rate tensor transport equation. A first approach to model a dissipation tensor transport equation has been made by Reynolds (1984). Later, Tagawa, Nagano & Tsuji (1991) proposed a dissipation rate tensor equation model in which they introduced closure assumptions for all unknown terms in the ε-tensor equation. Recently Speziale & Gatski (1997) developed a new dissipation rate tensor transport model. In a second step they invoked a local equilibrium hypothesis. This led to a scalar dissipation rate equation and an algebraic expression for the anisotropy of the dissipation rate tensor. Both the anisotropy of the dissipation rate tensor and the constant c_{ε_1} in the dissipation rate equation turn out to be nonlinear functions of the mean velocity gradient. This distinguishes it from many previously proposed scalar dissipation rate equations.

It has been argued by Speziale (1991) that it is more sound to base the turbulent macro-scale on the integral length scale rather than on the dissipation rate, which formally determines the turbulent microscale. In fact, the first complete Reynolds stress model was developed by Rotta (1951*a,b*) in combination with a scalar integral length-scale equation. He developed a length-scale transport equation by applying an integral operator to the trace of the two-point correlation equation in physical space. Wolfshtein (1971) has extended this approach to near-wall and low-Reynolds-number flows. In a more recent approach Besnard *et al*. (1990) developed a scalar length-scale equation starting from the two-point correlation function in spectral space. A similar approach has been followed by Aupoix (1987) in putting forward his MIS (Méthode Intégrale Spectrale) methodology. However, the MIS approach relies on the model of Lin & Wolfshtein (1979) which has been proven to be too oversimplified, as will be discussed below. Owing to the scalar character of the length-scale equations published in the literature, all the sink, source, and diffusion terms on the right-hand sides of the equations had to be modelled empirically.

To preserve the tensorial character of the two-point correlation equation and to avoid the large number of assumptions which significantly decreases the theoretical reliability of the length-scale equation, a few authors introduced the concept of a tensor length-scale equation. A preliminary suggestion for a tensor length scale has been made by Wolfshtein, Naot & Lin (1975). In a series of papers Donaldson and co-workers (Sandri 1977, 1978; Sandri & Cerasoli 1981; Donaldson & Sandri 1981) first developed a closed tensor length-scale equation. They approximated the correlation function R_{ij} as a delta function, leading to the elimination of some terms in the tensor length-scale equation. In addition, they used empirical models for several terms where exact terms can be calculated. Approximately at the same time but independent of Donaldson and co-workers, Lin & Wolfshtein (1979) developed a tensor length-scale equation. However, later it was shown by Kassinos & Reynolds (1990) that Lin & Wolfshtein neglected some fundamental terms in their approach.

Here, the route initiated by Rotta (1951*a,b*) will be followed. New information will be extracted from the two-point correlation tensor equations to develop a new Reynolds stress second-moment closure model. The final model consists of a dissipation rate tensor equation derived through a new length-scale tensor equation and an extended linear model for the pressure–strain correlation. Both the dissipation rate

tensor equation and the pressure–strain correlation account for compressibility effects in the limit of small Mach numbers.

In §2 a short introduction to the two-point correlation equations is given. In §3 the basic asymptotic limit and the tensor invariant model for the two-point correlation functions is introduced. Furthermore, a model for the triple-correlation will be developed. In the last subsection the tensor length-scale equation will be derived. In §4 the Kolmogorov relation between the turbulent kinetic energy, the dissipation rate and the integral length scale is extended to tensor-valued functions and a tensor dissipation rate equation is developed. In §5 a low-Mach-number compressibility extension of the linear pressure–strain model has been recast and turbulent transport models have been introduced. In §6 the model equations will be integrated numerically for four homogeneous and two inhomogeneous test cases. Model results will be compared with large-eddy simulation (LES), direct numerical simulation (DNS) and experimental data.

2. Governing equations

Consider the compressible Navier–Stokes equations in the limit of small Mach number. Splitting the velocity and pressure into their means $\bar{u}_i$, $\bar{p}$ and their fluctuations u_i, p the Reynolds-averaged Navier–Stokes and continuity equations are

$$\frac{\mathrm{D}\bar{u}_i}{\mathrm{D}t} = -\frac{\partial \bar{p}}{\partial x_i} + \nu \frac{\partial^2 \bar{u}_i}{\partial x_k \partial x_k} - \frac{\partial \overline{u_i u_k}}{\partial x_k} - 2 e_{ijk} \Omega_k \bar{u}_j, \tag{2.1a}$$

$$\frac{1}{\rho}\frac{\partial \rho}{\partial t} + \frac{\partial \bar{u}_k}{\partial x_k} = 0. \tag{2.1b}$$

In (2.1a) and subsequently $\mathrm{D}/\mathrm{D}t = \partial/\partial t + \bar{u}_k \partial/\partial x_k$ and $\overline{u_i u_j}$, ν and Ω_k are, respectively, the Reynolds stress tensor, the kinematic viscosity and the rotation rate of the coordinate system relative to an inertial frame. The density ρ is only a function of time and not subjected to the turbulent fluctuations. In (2.1a) the mean pressure $\bar{p}$ has been normalized with ρ.

To obtain a model for the Reynolds stress tensor $\overline{u_i u_j}$ the concept of two-point correlation will be introduced. The two-point one-time correlations are defined as

$$\left.\begin{aligned} R_{ij}(\boldsymbol{x}, \boldsymbol{r}, t) &= \overline{u_i(\boldsymbol{x}, t)\, u_j(\boldsymbol{x}^{(1)}, t)}, \\ R_{(ik)j}(\boldsymbol{x}, \boldsymbol{r}, t) &= \overline{u_i(\boldsymbol{x}, t)\, u_k(\boldsymbol{x}, t)\, u_j(\boldsymbol{x}^{(1)}, t)}, \\ \overline{pu_j}(\boldsymbol{x}, \boldsymbol{r}, t) &= \overline{p(\boldsymbol{x}, t)\, u_j(\boldsymbol{x}^{(1)}, t)}, \end{aligned}\right\} \tag{2.2}$$

which are functions of the physical and the correlation space coordinates x_k and $r_k = x_k^{(1)} - x_k$ respectively. The two-point correlation R_{ij} converges to the Reynolds stress tensor in the limit of zero separation r_k.

From the transport equation for the turbulent fluctuation velocity u_i the two-point correlation equation may be derived:

$$\begin{aligned} \frac{\mathrm{D}R_{ij}}{\mathrm{D}t} = & -R_{kj}\frac{\partial \bar{u}_i(\boldsymbol{x}, t)}{\partial x_k} - R_{ik}\frac{\partial \bar{u}_j(\boldsymbol{x}+\boldsymbol{r}, t)}{\partial x_k} - \left[\bar{u}_k(\boldsymbol{x}+\boldsymbol{r}, t) - \bar{u}_k(\boldsymbol{x}, t)\right]\frac{\partial R_{ij}}{\partial r_k} \\ & -\frac{1}{\rho}\left[\frac{\partial \overline{pu_j}}{\partial x_i} - \frac{\partial \overline{pu_j}}{\partial r_i} + \frac{\partial \overline{u_i p}}{\partial r_j}\right] + \nu\left[\frac{\partial^2 R_{ij}}{\partial x_k \partial x_k} - 2\frac{\partial^2 R_{ij}}{\partial x_k \partial r_k} + 2\frac{\partial^2 R_{ij}}{\partial r_k \partial r_k}\right] \\ & -\frac{\partial R_{(ik)j}}{\partial x_k} + \frac{\partial}{\partial r_k}\left[R_{(ik)j} - R_{i(jk)}\right] - 2\,\Omega_k\left[e_{kli}R_{lj} + e_{klj}R_{il}\right]. \end{aligned} \tag{2.3}$$

The divergence $\partial/\partial x_i - \partial/\partial r_i$ of the latter equation leads to a Poisson equation for $\overline{pu}_j$:

$$\frac{1}{\rho}\left[\frac{\partial^2\overline{pu_j}}{\partial x_k\partial x_k} - 2\frac{\partial^2\overline{pu_j}}{\partial r_k\partial x_k} + \frac{\partial^2\overline{pu_j}}{\partial r_k\partial r_k}\right]$$
$$= -2\left[\frac{\partial\bar{u}_k(\boldsymbol{x},t)}{\partial x_l} + e_{mlk}\Omega_m\right]\left[\frac{\partial R_{lj}}{\partial x_k} - \frac{\partial R_{lj}}{\partial r_k}\right] - \left[\frac{\partial^2 R_{(kl)j}}{\partial x_k\partial x_l} - 2\frac{\partial^2 R_{(kl)j}}{\partial x_k\partial r_l} + \frac{\partial^2 R_{(kl)j}}{\partial r_k\partial r_l}\right]. \quad (2.4)$$

The dependent variables in (2.3) and (2.4) have to satisfy the continuity conditions

$$\frac{\partial R_{ij}}{\partial x_i} - \frac{\partial R_{ij}}{\partial r_i} = 0, \qquad \frac{\partial R_{ij}}{\partial r_j} = 0, \quad (2.5a)$$

$$\frac{\partial R_{(ik)j}}{\partial r_j} = 0, \qquad \frac{\partial\overline{pu_i}}{\partial r_i} = 0. \quad (2.5b)$$

From geometrical considerations the remaining unknowns $R_{i(jk)}$ and $\overline{u_ip}$ are related to $R_{(jk)i}$ and $\overline{pu_i}$ by

$$R_{i(jk)}(\boldsymbol{x},t;\boldsymbol{r}) = R_{(jk)i}(\boldsymbol{x}+\boldsymbol{r},t;-\boldsymbol{r}) \qquad \text{and} \qquad \overline{u_ip}(\boldsymbol{x},t;\boldsymbol{r}) = \overline{pu_i}(\boldsymbol{x}+\boldsymbol{r},t;-\boldsymbol{r}). \quad (2.6)$$

It is worth mentioning that the only term to be modelled in the system (2.3)–(2.6) is the triple correlation $R_{(ik)j}$, to be discussed in §3.2. Equation (2.3) can be reduced to the Reynolds stress equations by introducing the limit $r_k \to 0$:

$$\frac{\mathrm{D}\overline{u_iu_j}}{\mathrm{D}t} = P_{ij} + \Phi_{ij} - 2\,\varepsilon_{ij} + D_{ij} + {}^{\nu}D_{ij} + C_{ij}, \quad (2.7)$$

where

$$P_{ij} = -\left[\overline{u_iu_k}\frac{\partial\bar{u}_j}{\partial x_k} + \overline{u_ku_j}\frac{\partial\bar{u}_i}{\partial x_k}\right], \quad \Phi_{ij} = \overline{\frac{p}{\rho}\left[\frac{\partial u_j}{\partial x_i} + \frac{\partial u_i}{\partial x_j}\right]},$$
$$\varepsilon_{ij} = \nu\overline{\frac{\partial u_i}{\partial x_k}\frac{\partial u_j}{\partial x_k}}, \quad D_{ij} = \frac{\partial}{\partial x_k}\left[-\overline{u_iu_ju_k} - \overline{p/\rho(u_i\delta_{jk} + u_j\delta_{ik})}\right],$$
$${}^{\nu}D_{ij} = \nu\frac{\partial^2\overline{u_iu_j}}{\partial x_k\partial x_k}, \quad C_{ij} = -2\,\Omega_k\left[e_{kli}\overline{u_ju_l} + e_{klj}\overline{u_iu_l}\right] \quad (2.8)$$

are, respectively, the production term, the pressure–strain correlation, the dissipation rate, the turbulent diffusion correlation, the viscous diffusion term, and the Coriolis term. In the Reynolds stress equations there are more functions to be modelled than in the two-point correlation equation. The information which is needed for the closure is contained in the two-point correlation equations. Within this approach, a model for a length-scale tensor $\mathscr{L}_{ij}$ will be derived, or alternatively the dissipation rate tensor ε_{ij} and the pressure–strain correlation Φ_{ij} will be modelled.

3. Derivation of the tensor length-scale equation

In order to obtain information about R_{ij}, without solving the system (2.3)–(2.6) in its full six-dimensional complexity, an integral form of equation (2.3) will be considered. The continuity equations (2.5*a*) are satisfied by introducing a tensor potential V_{mn} which is related to the correlation function R_{ij} by

$$R_{ij} = e_{ikm}\,e_{jln}\left[\frac{\partial}{\partial x_k} - \frac{\partial}{\partial r_k}\right]\frac{\partial V_{mn}}{\partial r_l}, \quad (3.1)$$

where e_{ijk} is the alternating tensor. For example, if isotropic turbulence is considered, the ansatz

$$V_{mn} = -\tfrac{1}{2}\,\overline{u^2}\,\delta_{mn}\int_0^r f(r)\,r\,\mathrm{d}r \quad \text{with} \quad r = |\boldsymbol{r}| \tag{3.2}$$

leads to the well-known result

$$R_{ij} = \overline{u^2}\left[\delta_{ij}\left(f + \tfrac{1}{2}rf'\right) - \frac{r_i\,r_j}{2\,r}f'\right], \tag{3.3}$$

first developed by von Kármán & Howarth (1938).

To preserve the tensorial character of the correlation function and to account for non-isotropic effects in R_{ij}, a generalization of (3.2) may be derived using tensor invariant theory (Spencer 1971). To avoid unclosed terms in the length-scale tensor equation and in the pressure–strain correlation the ansatz for V_{mn} should obey the following restrictions:

(i) V_{mn} is only a function of the correlation vector r_k and a new symmetric tensor $\int_0^r F_{mn}\,r\,\mathrm{d}r$,

(ii) V_{mn} is linear in the tensor $\int_0^r F_{mn}\,r\,\mathrm{d}r$,

(iii) V_{mn} has the dimension $\left[r^2 F_{mn}\right]$, where F_{mn} has the dimension of the Reynolds stress tensor.

Considering this, the most general formulation for V_{mn} contains eight independent tensor functions, as given in Appendix A and is an extension of the work by Naot *et al*. (1973). Three tensor forms become singular or cancel in the subsequent calculations. The remaining five are

$$\begin{aligned} V_{mn} = {} & \alpha_1\int_0^r F_{mn}\,r\,\mathrm{d}r + \alpha_2\,\delta_{mn}\int_0^r F_{kk}\,r\,\mathrm{d}r + \alpha_3\,\delta_{mn}\frac{r_k\,r_l}{r^2}\int_0^r F_{kl}\,r\,\mathrm{d}r \\ & + \alpha_4\frac{r_m\,r_n}{r^2}\int_0^r F_{kk}\,r\,\mathrm{d}r + \alpha_5\left[\frac{r_m\,r_k}{r^2}\int_0^r F_{nk}\,r\,\mathrm{d}r + \frac{r_n\,r_k}{r^2}\int_0^r F_{mk}\,r\,\mathrm{d}r\right]. \end{aligned} \tag{3.4}$$

The introduction of the potential function V_{mn} into (3.1) involves five coefficients α_1–α_5 which are not independent of each other. This is because the tensor F_{ij} has to obey an arbitrary, but fixed, one-point limit. Here, it is

$$\overline{u_i u_j} = R_{ij}(\boldsymbol{x}, t; \boldsymbol{r} = 0) = F_{ij}(\boldsymbol{x}, t; \boldsymbol{r} = 0), \tag{3.5}$$

which yields

$$\alpha_1 = 1 - \alpha_3 + \alpha_5 \quad \text{and} \quad \alpha_2 = \tfrac{1}{2}\left[-1 + \alpha_4\right]. \tag{3.6}$$

3.1. *Velocity correlation model and local homogeneity*

The basic assumptions for the subsequent derivation are two asymptotic limits. In the first one, it will be postulated that, to the leading order, each element of F_{ij} is solely a function of the absolute value of the correlation distance $\boldsymbol{r}$, but the dependence on the spatial coordinate $\boldsymbol{x}$ and the time t still remains. Thus,

$$F_{ij} = F_{ij}(\boldsymbol{x}, t; |\boldsymbol{r}|), \tag{3.7}$$

which is called a quasi-isotropic tensor. Introducing (3.4) into (3.1) by considering the limit (3.7), the final model for R_{ij} is obtained.

It has been shown by Oberlack, Rogers & Reynolds (1994), using a slightly modified form of (3.4), that the asymptotic limit (3.7) models the DNS data of a homogeneous shear flow to within a few per cent.

In turbulent flows sufficiently far away from solid walls, the variation in correlation space dominates the variation in physical space and hence a local homogeneity assumption of the two-point correlation equations (2.3)–(2.6) may be in order. Three parameters are defined which obey the following asymptotic limits:

$$\epsilon = \frac{l}{L} \ll 1, \quad \gamma = \frac{u'}{U} \ll 1 \quad \text{and} \quad Re_t = \frac{lu'}{\nu} \gg 1, \tag{3.8}$$

where l, L, u' and U are, respectively, characteristic measures of the integral length scale, an external body length scale, the fluctuation velocity and the mean velocity.

Close to solid walls ϵ, γ and Re_t may be of order one. Thus, (3.8) loses its validity and viscous effects may become dominant. Sufficiently far from the wall a consistent asymptotic expansion can only be established if $\varepsilon = \gamma$ and $1/(\varepsilon^2 Re_t) \to 0$ and the flow variables in the two-point correlation system (2.3)–(2.6) are expanded as

$$r_k = \xi_k \, \epsilon \tag{3.9}$$

and

$$\left.\begin{aligned} \bar{u}_i = \bar{u}_i^{(0)}(\boldsymbol{x}, t) + O(\epsilon), \;\; R_{ij} = \epsilon^2 R_{ij}^{(0)}(\boldsymbol{x}, t; \boldsymbol{\xi}) + O(\epsilon^3), \\ R_{(ij)k} = \epsilon^3 R_{(ij)k}^{(0)}(\boldsymbol{x}, t; \boldsymbol{\xi}) + O(\epsilon^4), \;\; \overline{pu_j} = \epsilon^3 \overline{pu_j}^{(0)}(\boldsymbol{x}, t; \boldsymbol{\xi}) + O(\epsilon^4). \end{aligned}\right\} \tag{3.10}$$

Using this in (2.3)–(2.6), the leading-order equations contain only x-derivatives with respect to the mean flow. The only exception is the convection term where the x-derivative with respect to R_{ij} still remains. Most important is that the non-local terms simplify to local derivatives. In the following the superscript $^{(0)}$ will be omitted.

3.2. *Closure of the triple correlation*

Any model for $R_{(ik)j}$ has to comply with (2.5*b*). Thus the triple correlation is expressed as a tensor potential $H_{(ik)m}$:

$$R_{(ik)j} = e_{jlm} \frac{\partial H_{(ik)m}}{\partial r_l}, \tag{3.11}$$

where $H_{(ik)m}$ has to be symmetric in the first two indices. It is assumed that the model for $H_{(ik)m}$ is solely a functional of the correlation distance r_k and the symmetric tensor F_{ij}. From this, a minimal integrity basis is composed to obtain a frame-invariant formulation for $H_{(ik)m}$. In general, this leads to eight terms by admitting only linear invariants of F_{ij} with the dimension $\left[r^2 F_{ij}\right]$ divided by an integral time scale. The eight terms are not all linearly independent. Hence, the following model is restricted to two terms plus a nonlinear isotropic turbulence model developed and tested previously by Oberlack, Peters & Kivotides (1991) and Oberlack & Peters (1992). The ansatz

$$H_{(ik)m}^{[1]} = \left[e_{mil} \, r_k + e_{mkl} \, r_i\right] \frac{r_l}{4\, r} K \tag{3.12}$$

leads to the isotropic form of $R_{(ik)j}$ first developed by von Kármán & Howarth (1938). For K Oberlack *et al*. (1991) have proposed

$$K = \frac{\sqrt{2}}{5(3\,\mathscr{C})^{3/2}} (2\,k - F_{jj})^{1/2} \frac{\partial F_{nn}}{\partial r}, \tag{3.13}$$

where $\mathscr{C}$ is the Kolmogorov constant and k is the turbulent kinetic energy. The new non-isotropic model is defined by

$$H_{(ik)m}^{[2]} = \beta_1 \, e_{mnl} \left[F_{in} \, r_k + F_{kn} \, r_i\right] \frac{r_l \, k^{3/2}}{\mathscr{L}_{jj}} + \beta_2 \left[e_{ilm} \, F_{lk} + e_{klm} \, F_{li}\right] \frac{r^2 \, k^{3/2}}{\mathscr{L}_{jj}}. \tag{3.14}$$

The expression $\mathscr{L}_{jj}$ is an integral of F_{jj}, as defined by (3.16) in the next subsection. The final model consists of the sum of the two terms $H^{[1]}_{(ik)m}$ and $H^{[2]}_{(ik)m}$. In §5 it will be shown that the non-isotropic model (3.14) leads to Rotta's return-to-isotropy model of the pressure–strain correlation (Rotta 1951*a*). Of course, the isotropic model does not contribute to the pressure–strain model.

3.3. *The tensor length-scale equation*

To derive a tensor length-scale equation, the integral operator

$$\psi(\cdot) = \frac{1}{4\pi}\int_{V_r}(\cdot)\,\frac{\mathrm{d}^3 r}{r^2} \tag{3.15}$$

introduced by Sandri (1977) will be applied to (2.3) in order to eliminate the correlation coordinate r_k. To make the quantity

$$\mathscr{L}_{ij} = \frac{1}{4\pi}\int_{V_r} F_{ij}\,\frac{\mathrm{d}^3 r}{r^2} \tag{3.16}$$

the new dependent transport variable, the remaining coefficients α_3–α_5 are rescaled to

$$a_1 = \frac{\alpha_3}{7}\frac{24}{5+3\alpha_3-5\alpha_5} \quad \text{and} \quad a_2 = \frac{1}{5}\frac{5+3\alpha_3-5\alpha_5}{1+3\alpha_4+2\alpha_5} \tag{3.17}$$

because only two of the parameters α_3–α_5 are linearly independent.

The following is a brief description of the derivation of the leading-order integrals in (2.3). Substituting R_{ij} by (3.1), (3.4) and (3.7), the quasi-isotropic tensor functions are evaluated using the formulas in Appendix B. As a result one obtains

$$\psi\left[R_{ij}\right] = \mathscr{L}_{ij}\left[\tfrac{2}{3}+\tfrac{2}{5}\alpha_3-\tfrac{2}{3}\alpha_5\right] + \delta_{ij}\mathscr{L}_{kk}\left[-\tfrac{2}{15}\alpha_3+\tfrac{2}{3}\alpha_4+\tfrac{2}{3}\alpha_5\right]. \tag{3.18}$$

In (2.3) the latter formula applies directly to both terms on the left-hand side and to the first two and the last term on the right-hand side. The evaluation of the last term in the first line of (2.3) and the calculating of the triple correlation may be carried out similarly while for the triple correlation the model (3.12)–(3.14) has been employed. Finally, to compute the integral of the pressure–velocity correlation $\overline{pu_j}$, (2.4) has been solved explicitly using the Green's function for an infinite domain, which to the leading order is

$$\overline{pu_j}(\boldsymbol{r}) = -\frac{\rho}{4\pi}\int_{V_{r^{(1)}}}\left[2\left(\frac{\partial\bar{u}_k}{\partial x_l}+e_{mlk}\Omega_m\right)\frac{\partial R_{lj}}{\partial r^{(1)}_k}-\frac{\partial^2 R_{(kl)j}}{\partial r^{(1)}_k\partial r^{(1)}_l}\right]\frac{\mathrm{d}^3 r^{(1)}}{|\boldsymbol{r}-\boldsymbol{r}^{(1)}|}. \tag{3.19}$$

Using this in (2.3), the application of the integral operator (3.15) results in a double space integral. Integration by parts and interchanging the order of the integration allows the evaluation of one volume integral. The remaining integral is given by

$$\psi\left[\frac{1}{\rho}\frac{\partial\overline{pu_j}}{\partial r_i}\right] = \frac{1}{4\pi}\int_{V_r}\left[2\left(\frac{\partial\bar{u}_k}{\partial x_l}+e_{mlk}\Omega_m\right)\frac{\partial^2 R_{lj}}{\partial r_k\partial r_i}-\frac{\partial^3 R_{(kl)j}}{\partial r_k\partial r_l\partial r_i}\right]\ln(|\boldsymbol{r}|)\mathrm{d}^3 r. \tag{3.20}$$

Using integration by parts again and introducing (3.1), (3.4), (3.5), and (3.7), the integral can be computed in the same manner as all the previous terms.

Collecting the integrals for each single term, an equation for the tensor length scale $\mathscr{L}_{ij}$ is derived. It contains $\delta_{ij}L_{kk}$ in the convection term as may be seen from (3.18). Taking the trace of this equation and subtracting it, after multiplication by δ_{ij} and a

certain factor from the previous tensor equation, the final tensor length-scale equation

$$\frac{\mathrm{D}\mathscr{L}_{ij}}{\mathrm{D}t} = {}^{1\mathscr{L}}P_{ij} + {}^{2\mathscr{L}}P_{ij} + {}^{\mathscr{L}}\Phi_{ij} - {}^{\mathscr{L}}E_{ij} + {}^{\mathscr{L}}C_{ij} \tag{3.21}$$

is obtained. Here

$${}^{1\mathscr{L}}P_{ij} = -\left[\mathscr{L}_{ik}\frac{\partial \bar{u}_j}{\partial x_k} + \mathscr{L}_{jk}\frac{\partial \bar{u}_i}{\partial x_k}\right], \tag{3.22a}$$

$${}^{2\mathscr{L}}P_{ij} = \left[\frac{2}{3} - \frac{28}{15}a_1a_2 - \frac{8}{15}a_2\right]\delta_{ij}\mathscr{L}_{kl}\frac{\partial \bar{u}_k}{\partial x_l} + \left[-\frac{1}{9} + \frac{8}{45}a_2 + \frac{28}{45}a_1a_2\right]\delta_{ij}\mathscr{L}_{kk}\bar{S}_{ll}, \tag{3.22b}$$

$$\begin{aligned}{}^{\mathscr{L}}\Phi_{ij} = {} & \left[\frac{2}{15} - \frac{1}{3a_2} + \frac{32}{15}a_1\right]\left[\bar{S}_{ij} - \frac{\delta_{ij}}{3}\bar{S}_{kk}\right]\mathscr{L}_{kk} + \left[\frac{2}{5} + \frac{56}{15}a_1\right]\left[\overline{W}_{ik}\mathscr{L}_{jk} + \overline{W}_{jk}\mathscr{L}_{ik}\right] \\ & + \left[-\frac{1}{5} + \frac{32}{15}a_1\right]\left[\mathscr{L}_{ij} - \frac{\delta_{ij}}{3}\mathscr{L}_{kk}\right]\bar{S}_{kk} \\ & + \left[\frac{4}{5} - \frac{16}{5}a_1\right]\left[\bar{S}_{ik}\mathscr{L}_{jk} + \bar{S}_{jk}\mathscr{L}_{ik} - \frac{2}{3}\delta_{ij}\bar{S}_{kl}\mathscr{L}_{kl}\right] \\ & - c_{\mathrm{R}}^{\mathscr{L}}\left[\frac{\mathscr{L}_{ij}}{\mathscr{L}_{kk}} - \frac{\delta_{ij}}{3}\right]k^{3/2},\end{aligned} \tag{3.22c}$$

$${}^{\mathscr{L}}E_{ij} = c_{\mathscr{L}}k^{3/2}\frac{\mathscr{L}_{ij}}{\mathscr{L}_{kk}}, \quad {}^{\mathscr{L}}C_{ij} = -2\Omega_k\left[e_{kli}\mathscr{L}_{jl} + e_{klj}\mathscr{L}_{il}\right]. \tag{3.22d,e}$$

The quantity $\mathscr{L}_{ij}$ divided by the kinetic energy has the dimension of a length scale. Equation (3.21) plays the role of a new length-scale equation in non-isotropic turbulence modelling and $\mathscr{L}_{ij}$ will therefore be referred to as a length-scale tensor function. The coefficients $c_{\mathrm{R}}^{\mathscr{L}}$ and $c_{\mathscr{L}}$ are functions of the parameters $\mathscr{C}$, β_1 and β_2. In (3.22) $\bar{S}_{ij}$ is the mean rate of strain, $\bar{\omega}_{ij}$ is the mean-vorticity tensor and $\overline{W}_{ij}$ is the absolute mean-vorticity tensor defined by

$$\bar{S}_{ij} = \frac{1}{2}\left(\frac{\partial \bar{u}_i}{\partial x_j} + \frac{\partial \bar{u}_i}{\partial x_j}\right), \quad \bar{\omega}_{ij} = \frac{1}{2}\left(\frac{\partial \bar{u}_i}{\partial x_j} - \frac{\partial \bar{u}_i}{\partial x_j}\right), \quad \text{and} \quad \overline{W}_{ij} = \bar{\omega}_{ij} + e_{mji}\,\Omega_m, \tag{3.23}$$

respectively.

To see the origin of each term in (3.22) it is convenient to trace back to the two-point correlation equation (2.3). The first production term ${}^{1\mathscr{L}}P_{ij}$ and the Coriolis term ${}^{\mathscr{L}}C_{ij}$ have clear counterparts in the first and last lines of (2.3). The second production term ${}^{2\mathscr{L}}P_{ij}$ and one part of the redistribution term ${}^{\mathscr{L}}\Phi_{ij}$ arise out of the last term in the first line of (2.3) which has no corresponding term in the Reynolds stress equation, because it vanishes in the limit of $r_k \to 0$. The major part of the redistribution term ${}^{\mathscr{L}}\Phi_{ij}$ originates from the pressure–velocity correlation, the first term in line two of (2.3). The latter and the sink term ${}^{\mathscr{L}}E_{ij}$ are the only terms that contain the model for the triple correlation. For second-moment closure, a frame-invariant and dimensionally correct relation between the tensor length-scale function $\mathscr{L}_{ij}$ and the dissipation rate tensor ε_{ij} is needed.

4. The dissipation rate tensor equation

In turbulence modelling on the level of second-moment closure models a dissipation rate or an integral length-scale equation are assumed to be an equivalent formulation

for the underlying physics. A familiar statement of this fact is the well-known scalar relation $\varepsilon \sim k^{3/2}/l$. A generalization of this relation to tensor notation should be an invariant formulation which relates the length-scale tensor function to the dissipation rate tensor.

Similar to the above scalar relation it is assumed that the length-scale tensor $\mathscr{L}_{ij}$ is only a function of the dissipation rate and the Reynolds stress tensor. The Cayley Hamilton theorem yields (Spencer 1971)

$$\mathscr{L}_{ij} = \frac{1}{2}\frac{k^{5/2}}{\varepsilon}\sum_{m,n=0}^{2}\varphi_{(m,n)}\left[b_{ik}^{m}\,d_{kj}^{n} + d_{ik}^{n}\,b_{kj}^{m}\right], \tag{4.1}$$

where b_{ij} and d_{ij} are the anisotropy parts of the Reynolds stress and the dissipation rate tensor, ε is the scalar dissipation rate and k is the turbulent kinetic energy, respectively,

$$b_{ij} = \frac{\overline{u_i u_j}}{2k} - \frac{\delta_{ij}}{3},\quad d_{ij} = \frac{\varepsilon_{ij}}{\varepsilon} - \frac{\delta_{ij}}{3},\quad \varepsilon = \varepsilon_{kk} \quad \text{and} \quad k = \frac{\overline{u_k u_k}}{2}. \tag{4.2}$$

In general, each $\varphi_{(m,n)}$ depends on the eight tensor invariants

$$\left.\begin{aligned} &\mathrm{II}_b = b_{kk}^2,\ \mathrm{III}_b = b_{kk}^3,\ \mathrm{II}_d = d_{kk}^2,\ \mathrm{III}_d = d_{kk}^3,\\ &\mathrm{I}_{bd} = b_{ij}d_{ji},\ \mathrm{II}_{bd} = b_{ij}^2 d_{ji},\ \mathrm{III}_{bd} = b_{ij}d_{ji}^2,\ \mathrm{IV}_{bd} = b_{ij}^2 d_{ji}^2. \end{aligned}\right\} \tag{4.3}$$

To leading order, $\mathscr{L}_{ij}$ is restricted to be a linear function of b_{ij} and d_{ij}. Thus, all nonlinear tensor products in (4.1) vanish and the remaining coefficients $\varphi_{(0,0)}$, $\varphi_{(1,0)}$ and $\varphi_{(0,1)}$ are constants. During the calibration process, $\varphi_{(1,0)}$ has been set equal to zero to avoid unrealizable results.

With the aid of (4.1), (3.21) may be converted to a dissipation rate tensor equation. From a computational point of view this is not necessary. However, it makes it easier to compare to other turbulence models which are usually proposed in conjunction with a dissipation rate equation. Taking the substantial derivative $\mathrm{D}/\mathrm{D}t$ of (4.1), one can derive a new tensor dissipation rate equation by replacing the substantial derivatives of the Reynolds stress $\overline{u_i u_j}$ and the tensor length scale $\mathscr{L}_{ij}$ by the right-hand sides of (2.7) and (3.21) respectively. This yields

$$\frac{\mathrm{D}\varepsilon_{ij}}{\mathrm{D}t} = {}^{1\varepsilon}P_{ij} + {}^{2\varepsilon}P_{ij} + {}^{\varepsilon}\Phi_{ij} - {}^{\varepsilon}E_{ij} + {}^{\varepsilon}C_{ij}. \tag{4.4}$$

Equation (4.4) contains four arbitrary constants: $a_0 = \varphi_{(0,0)}/(\varphi_{(0,1)}a_2)$, a_1, $c_{\mathrm{R}}^{\varepsilon}$ and c_{ε_2}: c_{ε_2} and $c_{\mathrm{R}}^{\varepsilon}$ are functions of the triple correlation model coefficients; c_{ε_2} has been set equal to 1.92 to match the limit of isotropic turbulence. The remaining three constants have been adjusted to some reference flows as will be seen in §6. The final form for each term in (4.4) then follows as

$${}^{1\varepsilon}P_{ij} = -\varepsilon_{ik}\frac{\partial \bar{u}_j}{\partial x_k} - \varepsilon_{jk}\frac{\partial \bar{u}_i}{\partial x_k}, \tag{4.5a}$$

$$\begin{aligned} {}^{2\varepsilon}P_{ij} = &-5\,\varepsilon_{ij}\frac{\overline{u_l u_k}}{2k}\frac{\partial \bar{u}_l}{\partial x_k} + \left[\frac{1}{9} - \frac{4}{135a_0}(2+7a_1)\right]\delta_{ij}\,\varepsilon\,\bar{S}_{kk}\\ &+ \frac{2}{15\,a_0}\left[\left(2\frac{\varepsilon_{ij}}{\varepsilon} - \frac{1}{3}\,\delta_{ij}\right)(4+14\,a_1) + 5\,a_0\,\delta_{ij}\right]\varepsilon_{kl}\frac{\partial \bar{u}_k}{\partial x_l}, \end{aligned} \tag{4.5b}$$

$$
\begin{aligned}
{}^{\varepsilon}\Phi_{ij} = {} & \left[\frac{7}{15} + \frac{32}{15}\,a_1 - \frac{8}{45a_0}(2+7a_1)\right]\bar{S}_{kk}\left[\varepsilon_{ij} - \frac{\delta_{ij}}{3}\varepsilon\right] \\
& + \left[\frac{2}{5} + \frac{56}{15}\,a_1\right]\left[\overline{W}_{ik}\varepsilon_{jk} + \overline{W}_{jk}\varepsilon_{ik}\right] + \left[\frac{2}{15} - a_0 + \frac{32}{15}\,a_1\right]\varepsilon\left[\bar{S}_{ij} - \frac{\delta_{ij}}{3}\bar{S}_{kk}\right] \\
& + \left[\frac{4}{5} - \frac{16}{5}\,a_1\right]\left[\bar{S}_{ik}\varepsilon_{jk} + \bar{S}_{jk}\varepsilon_{ik} - \frac{2}{3}\,\delta_{ij}\bar{S}_{kl}\varepsilon_{kl}\right] - c_{\mathrm{R}}^{\varepsilon}\,\frac{\varepsilon^2}{k}\,d_{ij}, \qquad (4.5c)
\end{aligned}
$$

$$
{}^{\varepsilon}E_{ij} = c_{\varepsilon_2}\,\frac{\varepsilon}{k}\varepsilon_{ij}, \quad {}^{\varepsilon}C_{ij} = -2\,\Omega_k\left[e_{kli}\,\varepsilon_{jl} + e_{klj}\,\varepsilon_{il}\right]. \qquad (4.5d,e)
$$

The production term ${}^{1\varepsilon}P_{ij}$ and the Coriolis term ${}^{\varepsilon}C_{ij}$ are consistent with the exact dissipation rate equation as they should be, since these are the only terms requiring no closure. The dilatational part of the production terms is consistent with rapid distortion theory in the limit of uniform compression.

The path which led to the dissipation rate tensor equation (4.4) is different from the direct approach introduced by Tagawa *et al*. (1991) or Speziale & Gatski (1997). Tagawa and coworkers closely followed the form of the classical scalar dissipation rate equation and modelled each single term separately. In their model they neglected a production term which may be important.

Speziale & Gatski divided all unclosed terms into 'rapid' and 'slow' and modelled them separately. The coefficient of the mean velocity gradient in the rapid terms may be written in terms of a generalized dissipation rate tensor $f_{ijkl} = 2\nu\overline{(\partial u_k/\partial x_i)(\partial u_l/\partial x_j)}$. The latter fourth-order tensor is modelled in terms of the dissipation rate tensor in the most general linear tensorially invariant form. Owing to the normalization and the symmetries of f_{ijkl}, the final model only contains one unknown constant similar to the rapid pressure–strain model in the Launder *et al*. (1975) (LRR) model. Speziale & Gatski's rapid model can be further divided into a part which contributes to the production and another which corresponds to the redistributes of the dissipation rate. Both terms correspond to, respectively, ${}^{2\varepsilon}P_{ij}$ and ${}^{\varepsilon}\Phi_{ij}$. The redistribution term has exactly the same form as in Speziale & Gatski and the sum of their production term models is very similar to ${}^{1\varepsilon}P_{ij} + {}^{2\varepsilon}P_{ij}$ in (4.5).

5. The pressure–strain correlation and turbulent transport model

The pressure–strain correlation Φ_{ij} which has the same order of magnitude as ε_{ij} can be tackled without additional closure assumptions by extending the work of Naot *et al*. (1973) to compressed turbulence.

As first shown by Chou (1945), the pressure–strain correlation Φ_{ij} can be expressed as an integral of the two-point correlation function

$$
\Phi_{ij} = \overline{\frac{p}{\rho}\left[\frac{\partial u_j}{\partial x_i} + \frac{\partial u_i}{\partial x_j}\right]} = \Phi_{ij_{\mathrm{rapid}}} + \Phi_{ij_{\mathrm{return}}} + \Phi_{ij_{\mathrm{surf}}}, \qquad (5.1)
$$

where

$$
\begin{aligned}
\overline{p\frac{\partial u_i}{\partial x_j}} = \frac{1}{4\pi}\int_{V_r}\Bigg[& 2\left(\frac{\partial \bar{u}_k}{\partial x_l}(\boldsymbol{x}+\boldsymbol{r}) + e_{mlk}\,\Omega_m\right)\left(\frac{\partial^2 R_{il}}{\partial x_j \partial r_k} - \frac{\partial^2 R_{il}}{\partial r_j \partial r_k}\right) \\
& + \left(\frac{\partial}{\partial x_j} - \frac{\partial}{\partial r_j}\right)\frac{\partial^2 R_{i(kl)}}{\partial r_k \partial r_l}\Bigg]\frac{\mathrm{d}^3 r}{|\boldsymbol{r}|} + \left.\overline{p\frac{\partial u_i}{\partial x_j}}\right|_{\mathrm{surf}}. \qquad (5.2)
\end{aligned}
$$

Model	c_1	c_2	c_3	c_4
LRR	0.8	1.31	1.75	–
GL	0.8	1.2	1.2	–
Present	0.8	0.8	2.4	−1.6

TABLE 1. Constants of the pressure–strain models

The surface integral $\Phi_{ij_{\text{surf}}}$ is relevant only near solid boundaries and thus has been neglected in the analysis. Introducing (3.1) into (5.2) and considering (3.4)–(3.10), the rapid term integral in (5.2) can be calculated and is given by

$$\begin{aligned}\Phi_{ij_{\text{rapid}}} = c_1 \left[\bar{S}_{ij} - \tfrac{1}{3}\delta_{ij}\bar{S}_{kk}\right] k + c_2 \left[\overline{W}_{ik} b_{jk} + \overline{W}_{jk} b_{ik}\right] k \\ + c_3 \left[\bar{S}_{jk} b_{ik} + \bar{S}_{ik} b_{jk} - \tfrac{2}{3}\delta_{ij}\bar{S}_{kl} b_{kl}\right] k + c_4\, b_{ij}\bar{S}_{kk}\, k,\end{aligned} \tag{5.3}$$

where

$$c_1 = \tfrac{4}{5}, \quad c_2 = \tfrac{4}{5} + 7\,a_3, \quad c_3 = \tfrac{12}{5} - 9\,a_3, \quad c_4 = -\tfrac{8}{5} + 6\,a_3, \quad a_3 = \tfrac{35}{16}\alpha_3. \tag{5.4}$$

The incompressible part of the rapid term model (5.3) has the same form as the LRR model and was first developed by Naot *et al*. (1973).

For comparison, the coefficients of the LRR and the Gibson & Launder (1978) models (GL) have been included in table 1. Apart from the coefficient c_1, which has been calculated by Crow (1968) using rapid distortion theory, the other constants in table 1 differ significantly from the present model which has been proposed with $\alpha_3 = 0$. The reason for the difference is twofold. First, most models are proposed in combination with a scalar dissipation rate equation and the anisotropy effects of the dissipation rate tensor are modelled as part of the slow pressure–strain correlation. Second, the modelling constants are usually fixed from experiments and thus other turbulence effects which are not separable from the pressure–strain correlation are included in their values.

Finally, introducing the model for the triple correlation (3.14) and (3.11) into (5.2), Rotta's well-known model (Rotta 1951*a*) for the return term of the pressure–strain correlation

$$\Phi_{ij_{\text{return}}} = -c_{\text{R}}\, \varepsilon\, b_{ij} \tag{5.5}$$

is recovered.

It should be emphasized that the basic assumption for the derivation of the length-scale equation (3.21) as well as for the pressure–strain correlation (5.3) is (3.7). It leads to an algebraic function for the pressure–strain correlation, which has been adopted in almost all second-moment closure models. In addition, using (3.7) avoids further unclosed terms in the tensor length-scale equation apart from the triple correlation function.

It can be shown that (3.7) is implicitly used in all nonlinear algebraic models for the pressure–strain correlation. Only the model for the tensor potential in (3.4) has to be extended to nonlinear tensor forms. Without restrictions like (3.7) for the correlation space dependence of R_{ij}, one has to solve a transport equation for (5.2) as has been shown by Oberlack (1994*b*) or a modified Hemholtz equation has to be solved as suggested by Durbin (1993).

For the calculation of the parabolic two-dimensional flows in the next section the turbulence model has been extended by adding a semi-empirical turbulent diffusion term to the Reynolds stress and the dissipation rate tensor transport equations (2.7)

and (4.4), respectively, which become

$$\frac{\mathrm{D}\overline{u_i u_j}}{\mathrm{D}t} = P_{ij} + \Phi_{ij} - 2\,\varepsilon_{ij} + C_{ij} + c_s \frac{\partial}{\partial x_k}\left[\frac{k}{\varepsilon}\overline{u_k u_l}\frac{\partial \overline{u_i u_j}}{\partial x_l}\right] \tag{5.6}$$

and

$$\frac{\mathrm{D}\varepsilon_{ij}}{\mathrm{D}t} = {}^{1\varepsilon}P_{ij} + {}^{2\varepsilon}P_{ij} + {}^{\varepsilon}\Phi_{ij} - {}^{\varepsilon}E_{ij} + {}^{\varepsilon}C_{ij} + c_\varepsilon \frac{\partial}{\partial x_k}\left[\frac{k}{\varepsilon}\overline{u_k u_l}\frac{\partial \varepsilon_{ij}}{\partial x_l}\right]. \tag{5.7}$$

The model constants in (4.5), (5.4) and (5.5) to be used in the subsequent computations are

$$\left.\begin{aligned} &a_0 = 0.05,\ \ a_1 = 0,\ \ c_{\mathrm{R}}^{\varepsilon} = 0.8,\ \ c_{\varepsilon_2} = 1.92,\\ &a_3 = 0,\ \ c_{\mathrm{R}} = 4,\ \ c_s = 0.0895,\ \ c_\varepsilon = 0.0688. \end{aligned}\right\} \tag{5.8}$$

In Oberlack (1994*a*), the constants c_ε and c_s have been chosen to meet the law of the wall. The remaining constants have been optimized previously in Oberlack (1994*b*) using homogeneous flows.

In the experiment of Maréchal (1972) there is some indication that the return to isotropy for the small scales may be similar to or faster than for the large scales. From the choice of c_{R} and $c_{\mathrm{R}}^{\varepsilon}$ it may appear that the return to isotropy of the Reynolds stresses is much faster than for the dissipation rate tensor. However, writing (5.6) and (5.7) in terms of b_{ij} and d_{ij} one sees that the actual coefficients of the return-to-isotropy terms are of the same order of magnitude.

The solid wall boundary conditions for $\overline{u_i u_j}$ and ε_{ij} have been made consistent with the logarithmic law of the wall and the constant-stress-layer assumption is imposed. The first computational point is chosen to lie in the log region. The Reynolds stresses and the dissipation rate tensor have been normalized with the shear stress velocity and the distance from the wall according to

$$\overline{u_i u_j} = u_\tau^2 \overline{u_i u_j}^*,\ \ \varepsilon_{ij} = \frac{u_\tau^3}{y}\varepsilon_{ij}^* \quad \text{with} \quad u_\tau = \left(\nu \left.\frac{\partial \bar{u}}{\partial y}\right|_w\right)^{1/2}, \tag{5.9}$$

where $\overline{u_i u_j}^*$ and ε_{ij}^* are constants. Employing this in (2.1), (5.6) and (5.7) a nonlinear set of algebraic equations for $\overline{u_i u_j}^*$ and ε_{ij}^* is obtained. In the actual computation of a wall-bounded flow the algebraic equations are solved in conjunction with (2.1), (5.6) and (5.7). The latter procedure has been employed for the computation of both the non-rotating and the rotating channel flow in §6.2.

6. Results

The dissipation rate tensor model has been tested using four independent homogeneous and two inhomogeneous two-dimensional test cases. In all test cases the Reynolds stress anisotropy is $b_{ij} = O(0.3)$ while the dissipation anisotropy is $d_{ij} = O(0.05)$

6.1. *Homogeneous turbulence subjected to constant mean velocity gradients*

In the following three subsections, §§6.1.1–6.1.3, homogeneous turbulence subjected to a constant mean velocity gradient is considered. All the initial conditions at $t = 0$ correspond to a state of isotropic turbulence where

$$b_{ij} = 0, \quad d_{ij} = 0, \quad k = k_0, \quad \varepsilon = \varepsilon_0. \tag{6.1}$$

Each of the following four test cases will be compared with the LES of Bardina *et*

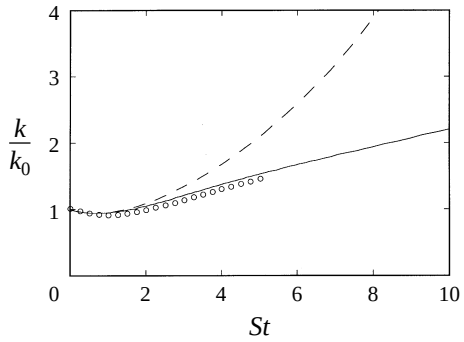

FIGURE 1. Evolution of the turbulent kinetic energy subjected to mean shear with $\varepsilon_0/(S\,k_0) = 0.18$: ———, present model; – – –, LRR model; ○, LES data of Bardina *et al*. (1983).

al. (1983) or with the DNS data of Lee & Reynolds (1985). The results of the widely used LRR model have also been included.

It can be shown that any solution for homogeneous shear flow with the initial conditions (6.1) depends only on the time-scale ratio $\varepsilon_0/(S\,k_0)$ where S is the inverse time scale of the mean flow defined in (6.2), (6.3) and (6.4) for each particular flow to be considered.

6.1.1. *Homogeneous shear turbulence*

The first homogeneous flow to be investigated is the homogeneous shear flow defined by the mean velocity gradient

$$\frac{\partial \bar{u}_i}{\partial x_j} = \begin{pmatrix} 0 & S & 0 \\ 0 & 0 & 0 \\ 0 & 0 & 0 \end{pmatrix}. \tag{6.2}$$

It can be seen from figure 1 that until $St \approx 1$ slow effects dominate the flow and the LRR as well as the new model capture the weak decrease of the turbulent kinetic energy. This trend is usually reproduced by common Reynolds stress models, but cannot be modelled by two-equation models. At about $St \approx 2$ the LRR model starts to deviate significantly from the weakly increasing curve given by the LES data. The present model is well in line with the entire set of LES data. This is an indication for the correct growth rate for large times even though no further data are provided.

6.1.2. *Homogeneous turbulence subjected to plane strain*

The second test case considers the evolution of the turbulent kinetic energy and the Reynolds stress anisotropy tensor for homogeneous plane strain. The mean velocity gradient is given by

$$\frac{\partial \bar{u}_i}{\partial x_j} = \begin{pmatrix} S & 0 & 0 \\ 0 & -S & 0 \\ 0 & 0 & 0 \end{pmatrix}. \tag{6.3}$$

As shown in figure 2(*a*), good agreement with the DNS data of Lee & Reynolds (1985) for both the LRR model and the present model is obtained. On the other hand, the corresponding non-zero components of the Reynolds stress anisotropy tensor in figure 2(*b*) are significantly better for the dissipation rate tensor model. In particular the tensor component b_{11} in the LRR model decreases, while the dissipation rate

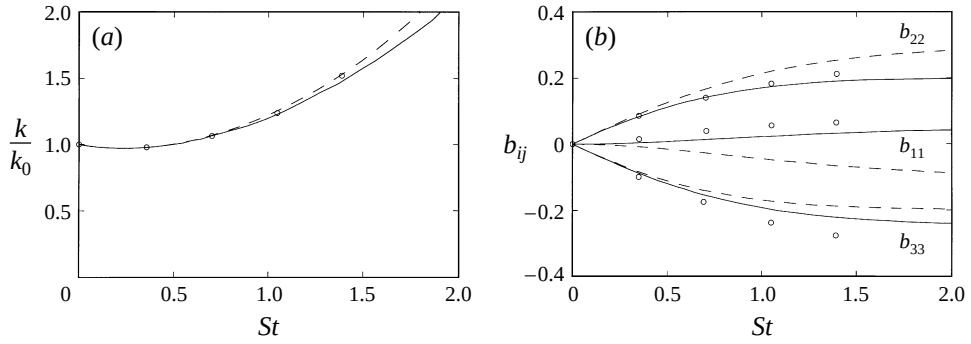

FIGURE 2. Evolution of the Reynolds stress tensor subjected to plane strain with $\varepsilon_0/(S\,k_0) = 0.25$: ———, present model; – – –, LRR model; ○, DNS data of Lee & Reynolds (1985). (*a*) Turbulent kinetic energy, (*b*) Reynolds stress anisotropy tensor.

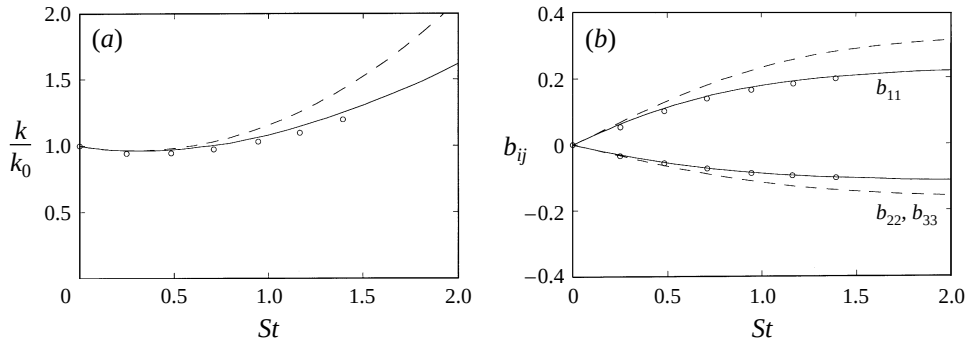

FIGURE 3. Evolution of the Reynolds stress tensor subjected to axisymmetric expansion with $\varepsilon_0/(S\,k_0) = 0.245$: ———, present model; – – –, LRR model; ○, DNS data of Lee & Reynolds (1985). (*a*) Turbulent kinetic energy, (*b*) Reynolds stress anisotropy tensor.

tensor model reproduces the trend of a weakly increasing b_{11} given by the DNS data.

6.1.3. *Homogeneous turbulence subjected to axisymmetric expansion and contraction*

The mean velocities for both test cases are three-dimensional, in contrast to the two flows considered above. The mean velocity gradients for the expansion and the contraction flow are, respectively, defined by

$$\frac{\partial \bar{u}_i}{\partial x_j} = \begin{pmatrix} -S & 0 & 0 \\ 0 & \frac{1}{2}S & 0 \\ 0 & 0 & \frac{1}{2}S \end{pmatrix} \quad \text{and} \quad \frac{\partial \bar{u}_i}{\partial x_j} = \begin{pmatrix} S & 0 & 0 \\ 0 & -\frac{1}{2}S & 0 \\ 0 & 0 & -\frac{1}{2}S \end{pmatrix}. \tag{6.4}$$

Again, the present model has been compared with the LRR model and with the DNS data of Lee & Reynolds (1985). From figures 3 and 4 it is clear that the dissipation rate tensor model performs much better than the LRR model and gives results which are almost identical to the DNS data.

6.2. *Turbulent channel flow in a rotating system*

To leading order, both the rotating channel flow and the turbulent plane jet are considered to have parabolic character and have been computationally treated as

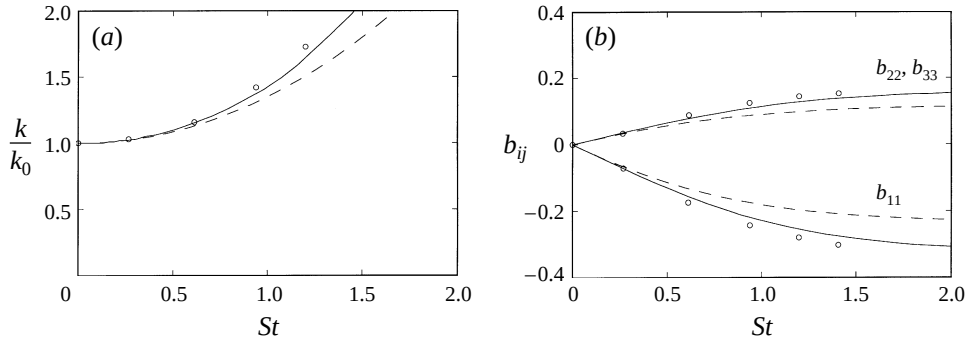

FIGURE 4. Evolution of the Reynolds stress tensor subjected to axisymmetric contraction with $\varepsilon_0/(S\,k_0) = 0.0179$: ——, present model; – – –, LRR model; ○, DNS data of Lee & Reynolds (1985). (*a*) Turbulent kinetic energy, (*b*) Reynolds stress anisotropy tensor.

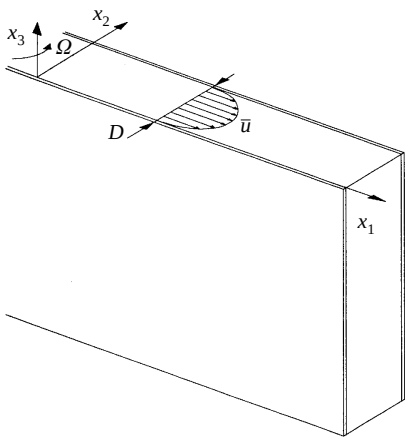

FIGURE 5. Flow configuration for the turbulent rotating channel flow.

such. The most reliable measurements of turbulent flow in a rotating channel flow are probably those carried out by Johnston, Halleen & Lazius (1972). Kristoffersen & Andersson (1993) have undertaken direct numerical simulations of the rotating turbulent channel flow for several different rotation numbers Ro where

$$Ro = \frac{\Omega D}{\bar{u}_m} \quad \text{with} \quad \bar{u}_m = \int_0^D \bar{u}_1(x_2)\,\mathrm{d}x_2. \tag{6.5}$$

A sketch of the flow geometry is given in figure 5.

The hydrostatic pressure due to the rotation can be absorbed into the mean pressure and hence does not appear explicitly in the equations. This is only valid for a constant rotation rate. As a result, the shear stress profile for $\overline{u_1 u_2} + \nu \partial \bar{u}_1/\partial x_2$ is linear with an arbitrary additive constant. In the non-rotating channel flow the variation is symmetric with respect to the channel axis, while in the rotating case the Coriolis forces in the Reynolds stress and in the dissipation rate tensor equation give rise to asymmetric profiles for all quantities. As a result, the wall shear stress is different for both sides. The flow on the pressure side ($x_2 = 0$) is destabilized, leading to an increase of the wall friction velocity u_{τ_D}. On the other hand, the turbulence on the suction side ($x_2 = D$) becomes stabilized which lowers the wall friction velocity

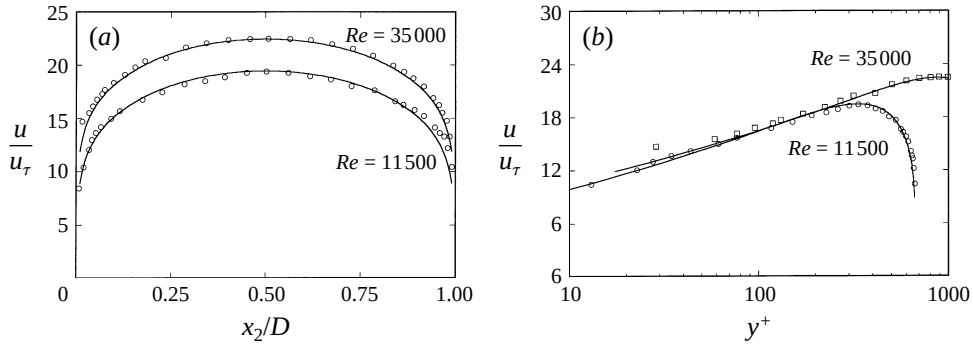

FIGURE 6. Mean velocity in a turbulent channel flow at $Ro = 0$: ———, present model; ○, experimental results of Johnston *et al*. (1972). (*a*) Linear scaling, (*b*) logarithmic scaling.

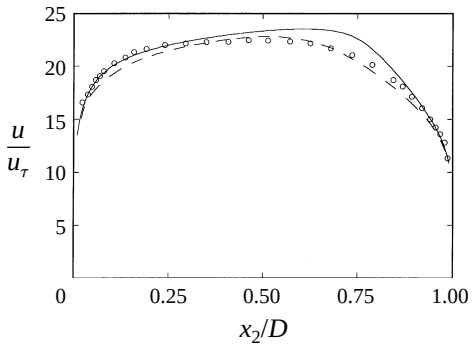

FIGURE 7. Mean velocity in a rotating turbulent channel flow at $Ro = 0.068$ and $Re = 35000$: ———, present model; – – –, Launder *et al*. (1987); ○, experimental results of Johnston *et al*. (1972).

u_{τ_S}. However, the total conservation of the wall friction is independent of the system rotation and thus the following relation holds:

$$u_\tau^2 = \tfrac{1}{2}\left(u_{\tau_D}^2 + u_{\tau_S}^2\right), \tag{6.6}$$

where u_τ is a constant. All quantities have been non-dimensionalized with u_τ and the channel width D.

The boundary conditions for the mean velocity and the turbulent quantities have been chosen according to the law of the wall and a constant-stress-layer assumption as explained in §5. Since no near-wall scaling law is known for the rotating case and the rotation number is small for all cases, the latter boundary condition has been adopted for all values of Ro. However, it should be stressed that no near-wall damping functions have been introduced.

In figures 6 and 7 the numerical results for the present model for zero and non-zero rotation numbers are compared with the experiments by Johnston *et al*. (1972). In figure 7 the results from the second-moment model by Launder, Tselepidakis & Younis (1987) have also been included. In the non-rotating test case the new dissipation rate tensor model and the experimental results are in good agreement. Some minor deviations are present for the rotating channel flow but the overall behaviour of $\bar{u}$ is reproduced very well. In the rotating case the model of Launder *et al*. produces slightly better results near the centreline while the present model performs better close to the walls. This is surprising since the present model has

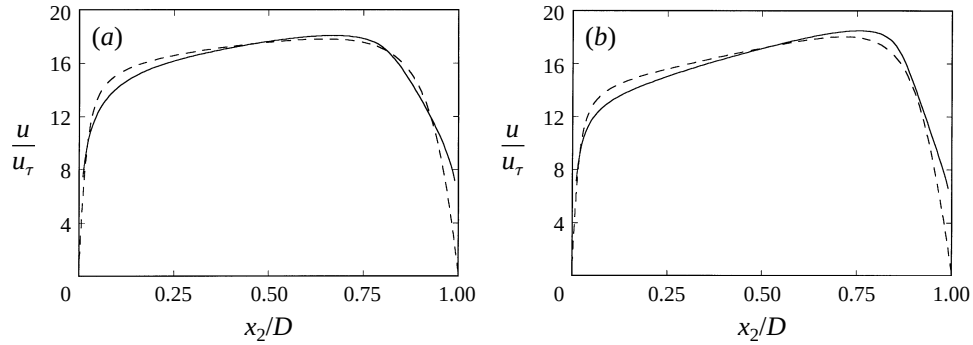

FIGURE 8. Mean velocity in a rotating turbulent channel flow: ——, present model; – – –, DNS data of Kristoffersen & Andersson (1993). (*a*) $Ro = 0.1$, (*b*) $Ro = 0.2$.

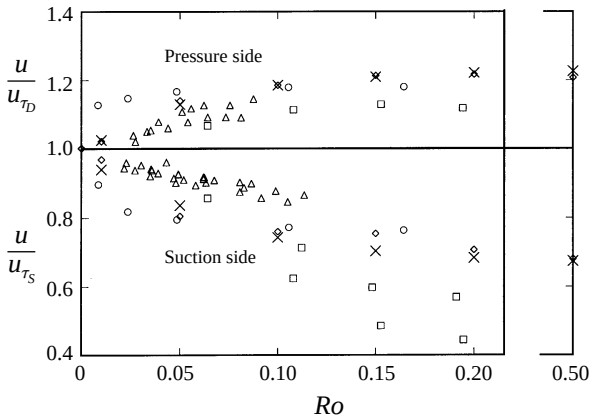

FIGURE 9. Wall friction velocities for the pressure and the suction side: ×, present model; ◇, DNS data of Kristoffersen & Andersson (1993); ○, LES data of Miyake & Kajishima (1986); experimental data of Johnston *et al*. (1972): □, $Re_m = 5500$; △, $23400 < Re_m < 36000$.

not been used in conjunction with a near-wall damping function while the model of Launder *et al*. makes use of it.

A second comparison of the turbulent channel flow has been made using the DNS data of Kristoffersen & Andersson (1993) at $Re = 5800$. In figure 8(*a,b*) mean velocities are shown for two different rotation numbers. In both cases the deviation from the DNS only amounts to a few percent but become slightly larger with increasing rotation number.

The last test case is the comparison of the wall friction velocities u_{τ_D} and u_{τ_S} from different computations and experiments as shown in figure 9. All the calculations reproduce the general experimental tendencies but the scatter amongst the results is large. The results from the present model follow closely the DNS data.

6.3. *The turbulent plane jet*

A classical inhomogeneous test problem for turbulence models is the turbulent plane jet. The flow is independent of any solid walls and the turbulence level at the edges of the jet has only a weak influence on the flow. A schematic picture of the flow geometry and the coordinate system is shown in figure 10.

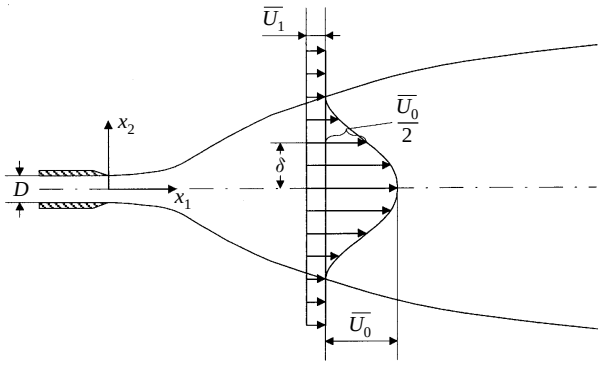

FIGURE 10. Schematic picture of the turbulent plane jet.

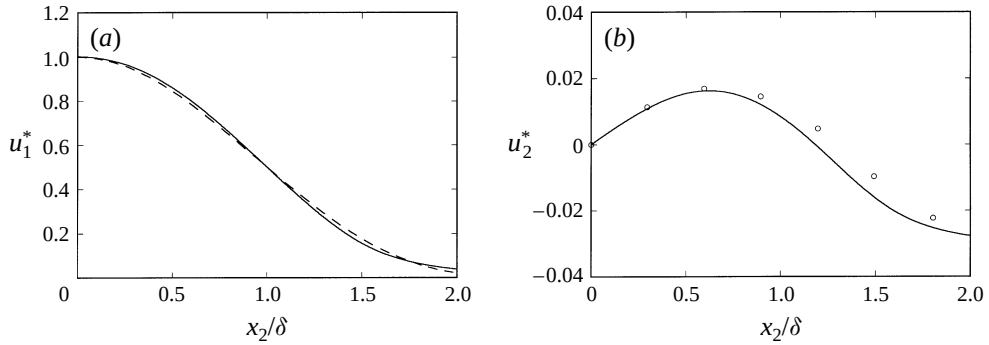

FIGURE 11. Mean velocities in a plane jet: ———, present model vs. the experimental results of Bradbury (1965) at a Reynolds number $Re_m = 30000$. (*a*) – – –, axial velocity, (*b*) ○, lateral velocity.

Experiments indicate that after the flow has developed for several nozzle diameters and if the velocity of the surrounding fluid is sufficiently low, the mean velocity converges to a self-similar profile. This has been used by Bradbury (1965) for the presentation of his experimental results assuming that the velocities are of the form

$$\bar{u}_1 = \bar{U}_1 + \bar{U}_0 \bar{u}_1^* \left(x_2/\delta\right) \quad \text{and} \quad \bar{u}_2 = \bar{U}_0 \bar{u}_2^* \left(x_2/\delta\right), \tag{6.7}$$

where $\delta = \delta(x_1)$ characterizes the jet width. The Reynolds stresses and the dissipation rate tensor are normalized as

$$\overline{u_i u_j} = \bar{U}_0^2 \overline{u_i u_j}^* \left(x_2/\delta\right) \quad \text{and} \quad \varepsilon_{ij} = \frac{\bar{U}_0^3}{\delta} \varepsilon_{ij}^* \left(x_2/\delta\right). \tag{6.8}$$

Bradbury has tested several different values for the outer flow velocity $\bar{U}_1$ and he has found no influence on the self-similarity of the mean velocities and the turbulent quantities. Following Bradbury, all the results in this subsection have been computed with $\bar{U}_1/\bar{U}_0 = 2\%$. The computation in the main flow direction was stopped at $200\delta_0$, where δ_0 is a characteristic jet width at the beginning of the calculation, and $200\delta_0$ corresponds to approximately 200 nozzle diameters for Bradbury's experiment. In the numerical calculation, the jet divergence in the main flow direction is very sensitive to the initial conditions. After a relative long distance downstream of the nozzle, the growth parameter δ/x_1 has converged to a value of 0.05 found by Bradbury.

In figure 11(*a*) the axial mean velocity computed with the dissipation rate tensor model is compared with Bradbury's data. The numerical result is in good agreement

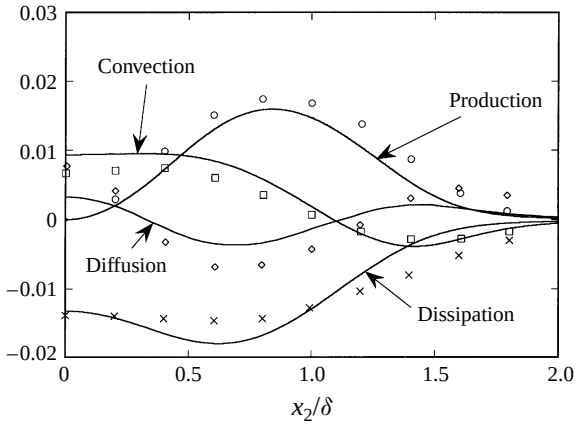

FIGURE 12. Balance in the turbulent kinetic energy equation: ———, present model; experimental data of Bradbury (1965) at $Re_m = 30000$; ○, production, □, convection; ◇, diffusion; ×, dissipation rate.

with the experiment and the relative error is within a few per cent. The functional form of the experimental result has been taken from Bradbury's curve fit. Similar small deviations from the experiments are seen in figure 11(*b*) for the lateral velocity.

As a final test, the turbulent kinetic energy balance from Bradbury's experiment is compared with the computation in figure 12. Experimental results for the statistical quantities, in particular for the turbulent transport and the dissipation, may not be very reliable compared to the mean flow data. However, global trends may be captured correctly and the model terms follow the experimental data very well.

7. Summary and conclusions

Using the two-point correlation equation a new tensor length-scale equation, or alternatively, a dissipation rate tensor equation was derived. In addition, a linear algebraic expression for the pressure–strain correlation from the two-point velocity correlation was developed. For the derivation of both the length-scale equation and the pressure–strain correlation two limits have been introduced, the stronger of which is to postulate that each component of a new two-point correlation tensor F_{ij} is only a function of the magnitude of the correlation distance. Using this, the two-point correlation function R_{ij} is written as a solenoidal tensor in terms of F_{ij} and the correlation distance vector r_k. Hence, directional information is employed due to the tensorial character of F_{ij} and the direction of the correlation distance. The second assumption is that of local homogeneity which is necessary to approximate the non-local behaviour of the two-point correlation equation. The final set of leading-order equations has a similar structure to the two-point correlation equations for homogeneous turbulence except that the convection term is still retained.

Employing both assumptions, a tensor length-scale equation has been derived by applying an integral operator to the two-point correlation equation. A non-isotropic model for the triple correlation is introduced, to achieve closure for the tensor length-scale equation. The resulting length-scale equation is in turn converted into a dissipation rate tensor equation by extending Kolmogorov's relation between the integral length scale, the dissipation rate and the turbulent kinetic energy. Both the equations for the tensor length-scale equation and the dissipation rate tensor

equation are valid for compressible turbulence in the limit of small Mach numbers. In contrast to common scalar dissipation rate equations the final equations can account for non-isotropic effects in the dissipation rate and for curvature or Coriolis force influences.

Similarly, introducing the two assumptions pointed out above into the integral representation of the pressure–strain correlation, an extended formulation for the linear rapid term was derived which also accounts for compressibility effects.

Of course, the model approach has its build-in limitations. Both assumptions used in the derivation of these equations are only asymptotically correct in the interior of a turbulent flow. Local homogeneity loses its validity close to solid walls because the turbulent and the mean scales become of the same order of magnitude and hence their ratio cannot be considered as small perturbation parameter. Furthermore, turbulence may become highly anisotropic near solid walls and thus the approach of a quasi-isotropic two-point correlation tensor is questionable.

To overcome the limitation of making the model only applicable to unbounded flows, a semi-empirical diffusion term has been added to the Reynolds stress transport equation and to the dissipation rate tensor equation. The model has been tested for four different homogeneous and two inhomogeneous turbulent flows.

Model results have been compared with DNS, LES and experimental data and the homogenous test cases have also be compared with the popular LRR model. Numerical results yield significant improvements for all of the homogeneous flows compared to the LRR model and some of the DNS and LES data are reproduced with a high accuracy. Even in some cases where the model deviates slightly from the DNS or LES data the correct trends are reproduced. In the case of the channel flow, which is the only wall-bounded flow, the mean velocities are computed with good accuracy. The results for the plane jet are also in good agreement with experiments and closely follow the experiments.

The author would like to thank Professor N. Peters for many helpful discussions and his great interest in the progress of the work. Improvements and comments on a draft of this paper by Dr D. A. Humphreys are gratefully acknowledged.

Appendix A. Some results on tensor invariant theory

In §3 the frame-invariant form is required expressing a symmetric second-order tensor in terms of the minimal number of terms consisting of a vector and another symmetric second-order tensor

$$V_{ij} = V_{ij}(\boldsymbol{r}, \mathscr{F}). \tag{A 1}$$

The basic idea for solving this problem is to contract (A 1) with two arbitrary vectors a_i and b_i. This reduces the problem to find all scalar invariants corresponding to

$$\Xi = \Xi(\boldsymbol{a}, \boldsymbol{b}, \boldsymbol{r}, \mathscr{F}). \tag{A 2}$$

Ξ can only be a linear function of a_i and b_i. The solution to the transformed problem is easier to determine and is given in Spencer (1971). For the modelling purpose in §3 the final form has been restricted to one linear in $\mathscr{F}_{ij}$. Considering this, the complete set of scalar invariants consists of the vector invariants

$$r_i r_i, \;\; a_i b_i, \;\; a_i r_i, \;\; b_i r_i, \;\; e_{ijk} a_i b_j r_k, \tag{A 3}$$

tensor invariant

$$\mathscr{F}_{kk}, \tag{A 4}$$

and mixed invariants

$$\left.\begin{array}{l} r_i\mathscr{F}_{ij}r_j,\ \ a_i\mathscr{F}_{ij}b_j,\ \ a_i\mathscr{F}_{ij}r_j,\ \ b_i\mathscr{F}_{ij}r_j,\ \ e_{ijk}r_i\mathscr{F}_{jl}r_la_k, \\ e_{ijk}r_i\mathscr{F}_{jl}r_lb_k,\ \ e_{ijk}a_i\mathscr{F}_{jl}b_lr_k,\ \ e_{ijk}r_i\mathscr{F}_{jl}a_lb_k,\ \ e_{ijk}a_i\mathscr{F}_{jl}r_lb_k. \end{array}\right\} \tag{A 5}$$

Next, all possible products of the system which are simultaneously linear in a_i and b_i have been composed. In the last step the vectors a_i and b_i are removed from the system and the final results yields

$$\begin{aligned} V_{ij} = {} & \alpha_1\mathscr{F}_{ij}r^2 + \alpha_2\delta_{ij}\mathscr{F}_{kk}r^2 + \alpha_3\delta_{ij}r_kr_l\mathscr{F}_{kl} + \alpha_4r_ir_j\mathscr{F}_{kk} + \alpha_5\left[r_ir_k\mathscr{F}_{jk} + r_jr_k\mathscr{F}_{ik}\right] \\ & + \alpha_6\frac{r_ir_jr_kr_l}{r^2}\mathscr{F}_{kl} + \alpha_7\left[e_{ilk}r_k\mathscr{F}_{lj} + e_{jlk}r_k\mathscr{F}_{li}\right]r \\ & + \alpha_8\left[r_ie_{klj}r_k\mathscr{F}_{lm}r_m + r_je_{kli}r_k\mathscr{F}_{lm}r_m\right]\frac{1}{r}. \end{aligned} \tag{A 6}$$

The last vector invariant in (A 3) and the last mixed invariant in (A 5) have not been considered in (A 6) because they imply a skew-symmetric tensor contribution to V_{ij}.

Furthermore, the last three terms in (A 6) were omitted from the calculation in §3 either because they do not contribute to the tensor length scale or because they lead to a singular integral.

Appendix B. Integrals of quasi-isotropic tensors

The following rules for the integration of quasi-isotropic tensor functions have been used for the derivation of the tensor length-scale equation in §3. Consider a scalar- or tensor-valued function T depending only on the spherical coordinate $r = |\boldsymbol{r}|$. Applying the integral operator

$$\Upsilon[\cdot] = \frac{1}{4\pi}\int_V(\cdot)\frac{\mathrm{d}^3r}{r^2} \tag{B 1}$$

to any quasi-isotropic function the following calculation rules apply provided the integrals are finite. If n is an odd number the integral of any quasi-isotropic tensors vanishes:

$$\Upsilon\left[r_{i_1}r_{i_2}\ldots r_{i_n}\frac{T(r)}{r^n}\right] = 0. \tag{B 2}$$

If n is an even number the integrals can be simplified. For $n = 2$ and 4 one obtains

$$\Upsilon^{(2)}\left[r_ir_j\frac{T(r)}{r^2}\right] = \tfrac{1}{3}\delta_{ij}\int_0^\infty T(r)\mathrm{d}r \tag{B 3}$$

and

$$\Upsilon^{(4)}\left[r_ir_jr_kr_l\frac{T(r)}{r^4}\right] = \tfrac{1}{15}\left[\delta_{ij}\delta_{kl} + \delta_{il}\delta_{jk} + \delta_{ik}\delta_{jl}\right]\int_0^\infty T(r)\mathrm{d}r. \tag{B 4}$$

All higher-order even integrants can be calculated recursively using

$$\Upsilon^{(n)}\left[r_{i_1}\ldots r_{i_n}\frac{T(r)}{r^n}\right] = \frac{1}{n+1}\sum_{k=2}^{n}\delta_{i_1i_k}\Upsilon^{(n-2)}\left[r_{i_2}\ldots r_{i_n}\frac{T(r)}{r_{i_k}r^{(n-2)}}\right]. \tag{B 5}$$

REFERENCES

Aupoix, B. 1987 Homogeneous turbulence two-point closures and applications to one-point closures. In *Special Course on Modern Theoretical and Experimental Approaches to Turbulent Flow Structures and its Modelling. AGARD Rep.* 755.

Bardina, J., Ferziger, J. H. & Reynolds W. C. 1983 Improved turbulence models based on large-eddy simulation of homogeneous, Incompressible Turbulent Flows. *Stanford University Tech. Rep.* TF-19.

Besnard, D. C., Harlow, F. H., Rauenzahn, R. M. & Zemach C. 1990 Spectral transport model for turbulence. *Los Alamos National Laboratory Rep.* LA-11821-MS.

Bradbury, L. J. S. 1965 The structure of a self-preserving turbulent jet. *J. Fluid Mech.* **23**, 31–64.

Brasseur, J. G. 1991 Comments on the Kolmogorov hypothesis of isotropy in the small scales. *AIAA* Paper 91-0230.

Brasseur, J. G. & Yeung, P. K. 1991 Large and small-scale coupling in homogeneous turbulence: Analysis of the Navier-Stokes equation in the asymptotic limit. In *Eighth Symp. Turbulent Shear Flows, Munich, Germany* 16-4-1.

Chou, P. Y. 1945 On velocity correlations and the solutions of the equations of turbulent fluctuations. *Q. Appl. Maths* **3**, 38–54.

Crow, S. C. 1968 Viscoelastic properties of fine-grained incompressible turbulence. *J. Fluid Mech.* **33**, 1–20.

Donaldson, C. duP. & Sandri, G. 1981 On the inclusion of information on eddy structure in second-order-closure models of turbulent flows. *AGARD Rep.* CP-308, pp. 25.1–25.14.

Durbin, P. 1993 A Reynolds stress model for near-wall turbulence. *J. Fluid Mech.* **249**, 465–498.

Durbin, P. & Speziale, C. G. 1991 Local anisotropy in strained turbulence at high Reynolds numbers. *Trans. ASME J. Fluids Engng* **117**, 707–709.

Gibson, M. M. & Launder, B. E. 1978 Ground effects on pressure fluctuations in the atmospheric boundary layer. *J. Fluid Mech.* **86**, 491–511.

Hallbäck, M., Groth, J. & Johansson, A. V. 1994 An algebraic model for nonisotropic turbulent dissipation rate in Reynolds stress closures. *Phys. Fluids* A **2**, 1859–1866.

Hanjalić, K. & Launder, B. E. 1972 A Reynolds stress model of turbulence and its application to thin shear flows. *J. Fluid Mech.* **52**, 609–638.

Johnston, J. P., Halleen, R. M. & Lazius, D. K. 1972 Effects of spanwise rotation on the structure of two-dimensional fully developed turbulent channel flow. *J. Fluid Mech.* **56**, 533–557.

Kármán, T. von & Howarth, L. 1938 On the statistical theory of isotropic turbulence. *Proc. R. Soc. Lond.* A **164**, 192–215.

Kassinos, S. C. & Reynolds, W. C. 1990 Tensorial volumes of turbulence revisited. *Phys. Fluids* A **2**, 1669–1677.

Kim, J., Moin, P. & Moser, R. 1987 Turbulence statistics in fully developed channel flow at low Reynolds number. *J. Fluid Mech.* **177**, 133–166.

Kolmogorov, A. N. 1941 The local structure of turbulence in incompressible viscous fluid for very large Reynolds numbers. *C.R. Acad. Sci. USSR* **30**, 301–305.

Kristoffersen, R. & Andersson, H. I. 1993 Direct simulations of low-Reynolds-number turbulent flow in a rotating channel *J. Fluid Mech.* **256**, 163–197.

Launder, B. E., Reece, G. C. & Rodi, W. 1975 Progress in the development of a Reynolds-stress turbulence closure. *J. Fluid Mech.* **68**, 537–566.

Launder, B. E., Tselepidakis, D. P. & Younis, B. A. 1987 A second-moment closure study of rotating channel flow. *J. Fluid Mech.* **183**, 63–75.

Lee, M. J. & Reynolds, W. C. 1985 Numerical experiments on the structure of homogeneous turbulence. *Stanford University Tech. Rep.* TF-24.

Lin, A. & Wolfshtein, M. 1979 Theoretical study of the Reynolds stress equations. In *Turbulent Shear Flows 1* (ed. F. Durst *et al.*). Springer.

Lin, A. & Wolfshtein, M. 1979 Tensorial volume of turbulence. *Phys. Fluids* **23**, 644–646.

Lumley, J. L. 1978 Computational modeling of turbulent flows. *Adv. Appl. Mech.* **18**, 123–176.

Lumley, J. L. & Newman, G. R. 1977 The return to isotropy of homogeneous turbulence. *J. Fluid Mech.* **82**, 161–178.

Maréchal, J. 1972 Étude expérimentale de la déformation plane d'une turbulence homogène. *J. Méc.* **11**, 263–294.

Miyake, Y. & Kajishima, T. 1986 Numerical simulation of the effects of Coriolis force on the structure of turbulence. *Bull. JSME* **29**, 3341–3351.

Naot, D., Shavit, A. & Wolfshtein, M. 1973 Two-point correlation model and the redistribution of Reynolds stress. *Phys. Fluids* **16**, 738–743.

Oberlack, M. 1994*a* Herleitung und Lösung einer Längenmaß- und Dissipations-Tensorgleichung für turbulente Strömungen. PhD thesis, RWTH Aachen, VDI Düsseldorf.

Oberlack, M. 1994*b* Closure of the dissipation tensor and the pressure–strain tensor based on the two-point correlation equation. In *Turbulent Shear Flows 9* (ed. F. Durst *et al.*). Springer.

Oberlack, M. & Peters, N. 1992 Closure of the two-point correlation equation as a basis of Reynolds stress models. *Appl. Sci. Res.* **51**, 533–538.

Oberlack, M., Peters, N. & Kivotides, D. 1991 Solutions of the von Kármán–Howarth equation by gradient flux approximations. *Eighth Symp. Turbulent Shear Flows,* pp. III-12-1.

Oberlack, M., Rogers, M. M. & Reynolds, W. C. 1994 Modeling the two-point correlation of the vector stream function. In *Studying Turbulence Using Numerical Databases – V, Center for Turbulence Research, Proceedings of the Summer Program.*

Reynolds, W. C. 1984 Physical and analytical foundations, concepts, and new directions in turbulence modeling and simulations. In *Turbulence Models and their Applications.* Editions Eyrolles, 61 Bd Saint-Germain Paris 2.

Rotta, J. C. 1951*a* Statistische Theorie Nichthomogener Turbulenz, 1. Mitteilung. *Z. Phys.* **129**, 547–572.

Rotta, J. C. 1951*b* Statistische Theorie Nichthomogener Turbulenz, 2. Mitteilung. *Z. Phys.* **131**, 51–77.

Saddoughi, S. G. & Veeravalli, S. V. 1994 Local isotropy in turbulent boundary layers at high Reynolds number. *J. Fluid Mech.* **268**, 333–372.

Sandri, G. 1977 A new approach to the development of scale equations for turbulent flows. *ARAP Rep.* 302.

Sandri, G. 1978 Recent results obtained in the modeling of turbulent flows by second-order closure. *AFOSR* TR-78-0680.

Sandri, G. & Cerasoli, C. 1981 Fundamental research in turbulent modeling. *ARAP Rep.* 438.

Spencer, A. J. M 1971 Theory of invariants. In *Continuum Physics* (ed. A. C. Eringen), vol. 1, pp. 239–353.

Speziale, C. G. 1991 Analytical methods for the development of Reynolds-stress closures in turbulence. *Ann. Rev. Fluid Mech.* **23**, 107–157.

Speziale, C. G. & Gatski, T. B. 1997 Analysis and modelling of anisotropies in the dissipation rate of turbulence. *J. Fluid Mech.* **344**, 155–180.

Tagawa, M., Nagano, Y. & Tsuji, T. 1991 Turbulence model for the dissipation components of reynolds stresses. In *Eighth Symp. Turbulent Shear Flows, Munich, Germany* 29-3-1.

Tavoularis, S. & Corrsin, S. 1984 Analytical methods for the development of Reynolds–stress closures in turbulence. *J. Fluid Mech.* **104**, 311–347.

Wolfshtein, M. 1971 On the length-scale-of-turbulence equation. *Isr. J. Technol.* **8**, 87–99.

Wolfshtein, M., Naot, D. & Lin, A. 1975 Models of turbulence. In *Topics in Transport Phenomena, Bioprocesses, Mathematical Treatment Mechanisms* (ed. C. Gutfinger). Hemisphere.